Hydrogen-bond Assisted Formation of Rod Shaped Organic Nanocrystals: Control of the Aggregational State and Structural Elucidation

Dong, B.; Galka, C.H.; Gade, L.H.; Chi, L.; Williams, R.M.

[Link to publication](#)

Hydrogen-bond Assisted Formation of Rod Shaped Organic Nanocrystals: Control of the Aggregational State and Structural Elucidation

Bin Dong, [1,2] Christian H. Galka,[3] Lutz H. Gade,[3,*] Lifeng Chi[1,2,*] and René M. Williams[4,*]

[1] Physikalisches Institut, Westfälische Wilhelms-Universität Münster & Center for Nanotechnology (CeNTech), 48149 Münster, Germany
[2] Key lab for supramolecular structure and materials, College of Chemistry, Jilin University, 130023 Changchun, P. R. China
[3] Anorganisch-Chemisches Institut, Im Neuenheimer Feld 270, 69120 Heidelberg, Germany
[4] Molecular Photonics Group, Van't Hoff Institute for Molecular Science (HIMS) Universiteit van Amsterdam, Nieuwe Achtergracht 129, 1018 WV Amsterdam, The Netherlands

Abstract. Rod-shaped nanocrystals are formed by self assembly of *t*-Bu-phenyl substituted tetra(carboxamido)perylenes (BPP) in different solvents. The structure and the dimensions of the nano-rods may be controlled by the choice of the hydrogen-bond accepting capacity of the solvent (DMSO, DMF, DMAc, HMPA), by the concentration and by the composition of solvent-mixture (by adding hydrogen-bond donating solvents), but is independent of the surface used for their deposition (mica, silicon, gold, glass). The different forms of aggregation were examined by AFM and SNOM and were correlated to UV-Vis absorption spectra of the aggregates in solution. The orientation of the transition dipole moment of the molecules in the nanocrystals has been determined by polarized fluorescence microscopy and, in combination with the crystal structure of the *t*-Bu substituted analogue of BPP, is used to develop a model for the internal molecular structure of the rod shaped aggregates.

Introduction

Nanostructured materials range from noble metals [1, 2], inorganic oxides [3], semiconductors [4] to purely organic compounds [5] and this exciting research field is fueled by a wide variety of applications in the coating industry and in medicine [6] as well as in the development of electronic and

* E-mail: williams@science.uva.nl, chi@uni-muenster.de, lutz.gade@uni-hd.de

photonic devices [7, 8] such as field effect transistors or photonic wires. Compared with the wide variety of inorganic nanostructures, organic aggregates have been studied somewhat less extensively in terms of their methods of preparation and physicochemical properties. Organic dye molecules are able to interact in such a way that organization is induced, either by a phase transition or by self-assembly. The 'reprecipitation method', an injection method, developed by Nakanishi et al. [9] has been employed to induce controlled crystallization at the nano- to micro-meter scale of compounds such as perylene and p-terphenylene. Using this method in combination with surfactants, it has been possible to create rod type structures of perylene [9d].

Using self-assembly [10] to create nanoscopic structures, i.e. the assembly based on the well-defined interaction of functional groups, has the advantage of allowing for a certain level of direct control in the aggregation process. The ordered assemblies may bridge the gap between the single molecule and structurally ordered macroscopic crystals and may display unique properties [11] (e.g. giant oscillator strength, excitonic coherence). Several attempts to control the formation of organic molecular aggregates with a regular shape through self-assembly have been made [12].
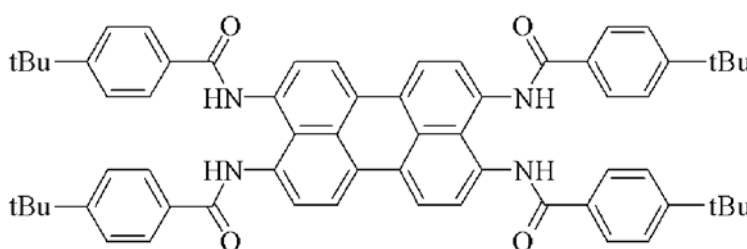

Fig. 1. The molecular structure of the *t-butyl-phenyl substituted* tetra-carboxamido perylene "BPP"

Herein, we wish to report on the control of the aggregational state of a new type of rod-shaped nanoscale aggregates and their characterization. The compound employed is a *t*-Bu-phenyl substituted tetra-(carboxamido) perylene (abbreviated as BPP, see *Fig. 1*) the synthesis of which we reported previously [13a]. BPP is a derivative of 3,4,9,10-tetraaminoperylene [13b–c] in which the peripheral amino functions have been transformed to amides in order to stabilize the reduced "perylenic" form of the molecule and to allow for directed intermolecular interactions through hydrogen bonding. In fact, we found that the hydrogen bonds of the amide groups are quintessen-

tial for the spontaneous formation of the large-organized structures. In this respect, intramolecular hydrogen-bonding confers rigidity to the molecules whereas intermolecular hydrogen bonding between the amide groups and hydrogen-bond accepting solvents appears to determine the outcome of the assembly process. A combination of synthetic organic chemistry, UV-Vis-spectroscopy and scanning probe microscopy is thus required to study these nano-assemblies. The materials studied in this work may prove useful for the generation of electronic and photonic devices that contain supramolecular self-assembled nano-rods as functional components.
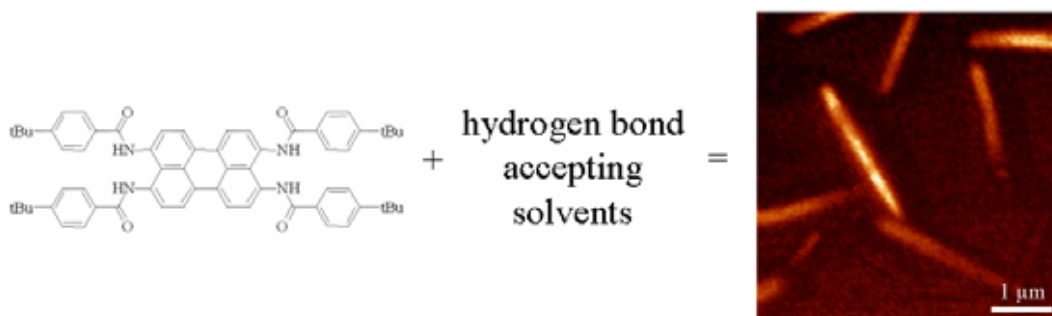
Experimental section

The synthesis of *t*-Bu-phenyl substituted tetra-(carboxamido) perylene (BPP) has been described previously [13a]. Dimethylsulfoxide (DMSO), dimethylformamide (DMF), dimethylacetamide (DMAc), hexamethylphosphoramide (HMPA) and dichloromethane (DCM) were purchased from Aldrich Company (in spectroscopy grade if available) and used without further purification. The UV-Vis measurements were performed on a Hewlett Packard 8453 diode array spectrophotometer while the polarized fluorescence images were recorded on a Zeiss Axioplan Microscope. The SNOM (Scanning Near-field Optical Microscopy) image was obtained on a home-built machine with a triangular tip [14]. The AFM images were recorded on a Multimode AFM, (Digital Instrument) with silicon tips (resonance frequency in the range of 280–330 KHz). The nano-rod samples for AFM, SNOM and polarized fluorescence microscope characterization were prepared by casting one drop of solution containing BPP onto a substrate (mica, silicon, gold, etc.) and subsequent evaporation of the solvent in vacuo.

Results and discussion

UV-Vis absorption spectroscopy

We were able to test the influence of a large number of solvents with various hydrogen-bond accepting capacities on the aggregational behavior of BPP, due to the fact that the color of a solution of BPP gives a good indication of the aggregational state of the molecules, as we have reported previously [13a]. By this procedure it was found that the typical yellow/reddish color of the solutions, indicating the presence of monomeric dye molecules, was observed in most solvents (e.g. nitro-methane, CS_2, pyridine). On the other hand, the distinct magenta or blue color, which is indicative of the formation of the nanocrystals, only appeared in strongly hydrogen-bond accepting solvents such as DMSO, DMF, DMAC and HMPA. Furthermore we found the magenta or blue color of the solution of aggregated BPP changed into the monomeric yellow color by either sonication or the addition of a small amount of protic solvents such as water or alcohol. These wet yellow colored solutions can be reversibly converted back to magenta or blue solution by means of storing at higher temperature (75°C) or adding molecular (drying) sieves at room temperature. In both cases, the lighter boiling protic solvent is removed from the solution either by evaporation or by trapping in the molecular sieves. The spectral changes that are due to these solvent effects and the accompanying treatments are represented in *Fig. 2.*

   The UV-Vis absorption spectrum of the yellow monomeric form of BPP in DCM (maxima at 316 nm, 332 nm, 410 nm and 434 nm) as well as the spectrum in DMSO (maxima at 573 and 780 nm) and in HMPA (maxima at 573, 616, 746 and 842 nm) are depicted in *Fig. 2a.* As described below, these spectra can be correlated with different types of aggregational states (see AFM results). The absorption spectra of the solutions containing the nanocrystalline aggregates are strongly red-shifted compared to those of the monomeric form, indicating that the carboxamido perylene monomer can self-assemble into special J-type aggregates which are probably induced by hydrogen bonding with the solvent molecules. The effect of sonication is shown in *Figure 2b,* in which the spectral changes are attributed to the de-aggregation of the "Scheibe polymers". By addition of a small amount of a hydrogen-bond donating solvent (e.g. water or methanol) to a solution of the molecular aggregate, similar observations (breaking of the aggregates into monomer form) can be made, therefore confirming the role of the hydrogen-bond accepting capacity of the solvent in the formation of the aggregate. In other words, hydrogen bond accepting solvents assist the rod-

formation whereas hydrogen bond donating solvents work in the opposite direction. This finding is remarkable and in contrast to the fact that many J-aggregates only exist in hydrogen-bond donating solvents (e.g. water, alcohol) at a high concentration [15]. Furthermore, J-aggregates tend to collapse thermally [16], which is not observed for the BPP rods.
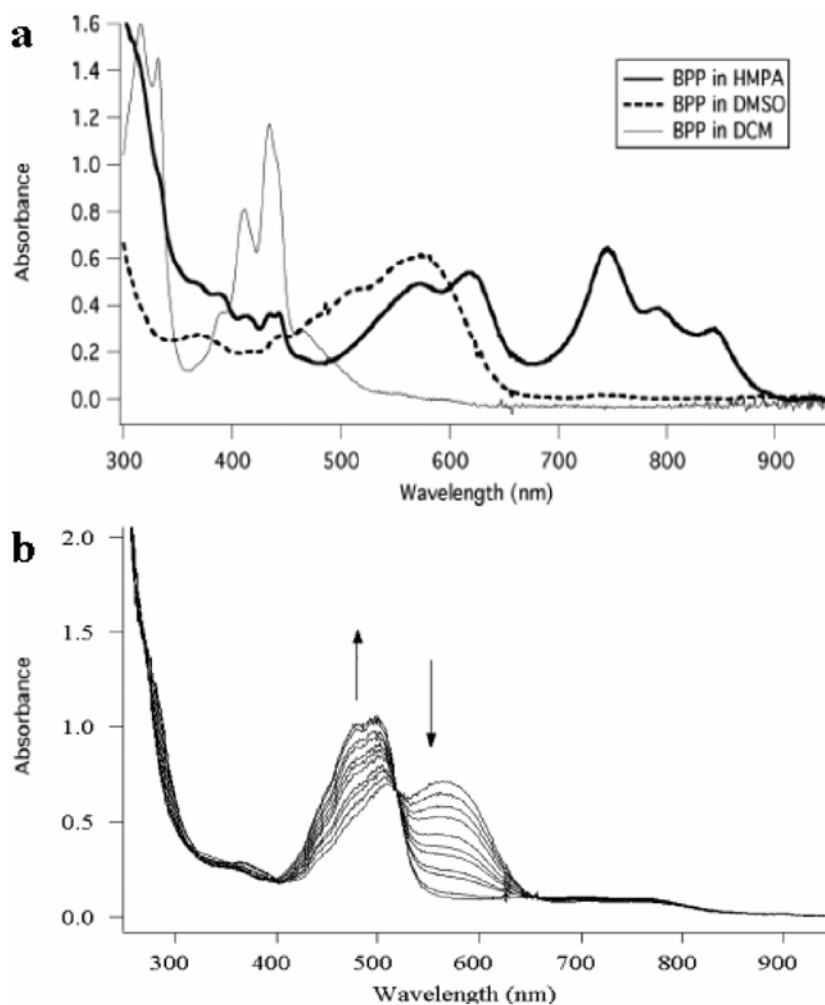

Fig. 2. (*a*) Comparison of the UV-Vis spectral features of monomeric BPP in dichloromethane (DCM), the nanocrystals in DMSO, which have a length of ~300 nm and the nanocrystals in HMPA solution which are ca. 2 μm long. (*b*) Effects of sonication of a solution of nanocrystals in DMSO. Consecutive spectra were taken after periods of sonication of 5 seconds
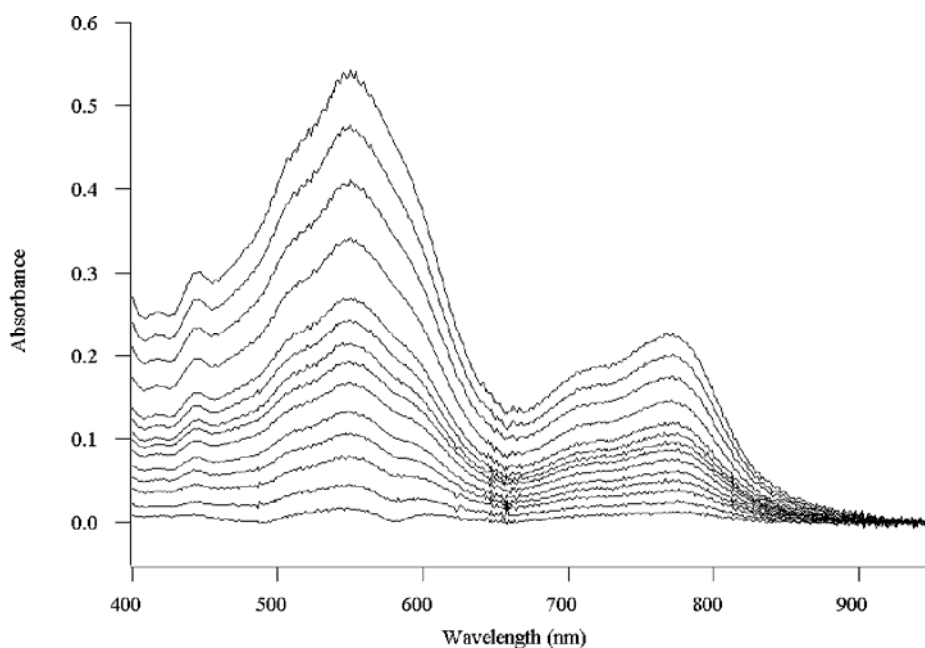
Fig. 3. Set of absorption spectra of DMSO solutions of BPP at various concentrations of: 1.46 × 10^{-5} (lowest spectrum), 2.92×10^{-5}, 4.38×10^{-5}, 5.84×10^{-5}, 7.3×10^{-5}, 8.76×10^{-5}, 1.02×10^{-4}, 1.17×10^{-4}, 1.31×10^{-4}, 1.46×10^{-4}, 1.83×10^{-4}, 2.19×10^{-4}, 2.55×10^{-4} to 2.92×10^{-4} M (upper spectrum)

The concentration dependence of the absorption spectrum of aggregated BPP was studied and the absorption spectra of a DMSO solution of BPP at different concentrations are displayed in *Fig. 3*. These undergo negligible spectral changes upon varying the concentration, indicating that the concentration effects observed in the AFM (vide infra) are due to coagulation of smaller rod shaped aggregates upon solvent evaporation. Notably, BPP can form aggregates at very low concentration (10^{-5} M), and the features of the monomer spectra never appear, regardless of how low the concentration is.

AFM characterization

The perylene dye aggregates formed in solution and subsequently deposited on a substrate were examined by AFM. For solutions of monomeric BPP molecules (either in DCM or in DMSO with a small amount of added water) we observe only featureless structures, indicating the absence of mo-

lecular organization. In contrast, for all hydrogen bond accepting solvents used (DMSO, DMF, DMAc and HMPA), we observed the nano-rod structures depicted in *Fig. 4*.
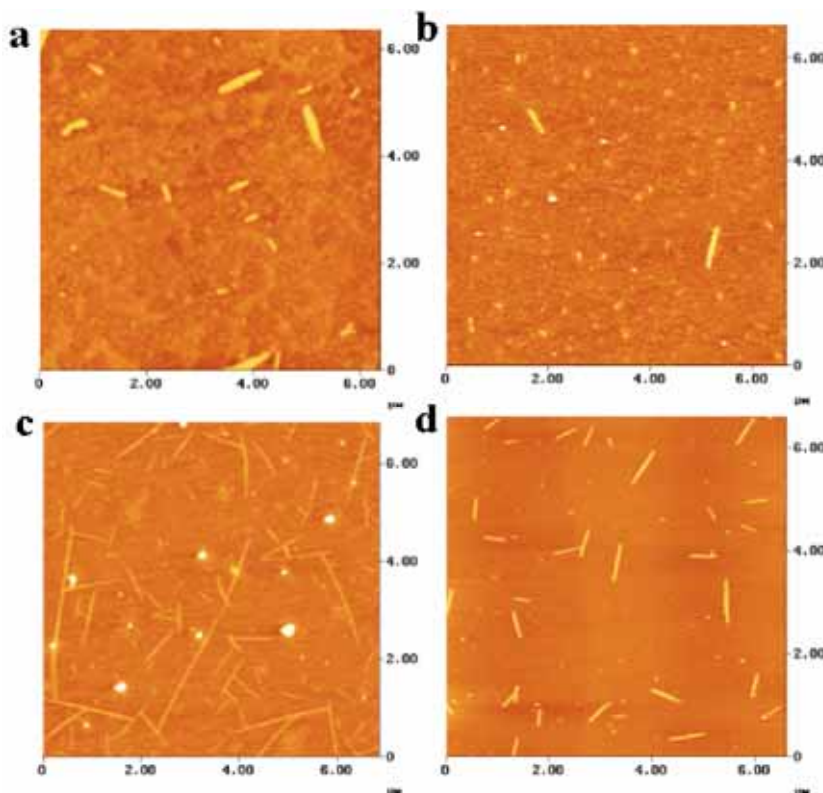

Fig. 4. AFM images of the BPP aggregates deposited on mica from different solvents (2×10^{-5} M): (*a*) DMAc (*b*) DMF (*c*) HMPA (*d*) DMSO

The hydrogen-bond accepting capacity of the solvents appears to affect the size and structure of the nano-rods formed in solution. For example, the aggregates observed in HMPA (strong hydrogen-bond acceptor) are apparently longer and thinner (1 nm in thickness in comparison with 2 nm, see *Fig. 4c*) than in the other solvents, whereas the overall amount of the nano-rods formed in DMF (weak hydrogen-bond acceptor) is apparently less. The formation of the nano-rod shaped aggregates is not influenced by the substrate upon which they are deposited (crystalline or amorphous, molecularly flat or irregular) indicating the aggregate formation originates from the interactions between the BPP molecules and solvent (and not with the sub-

strate). In *Fig. 5* the nano-rods deposited from DMSO solution on silicon, glass, mica, and gold surfaces are displayed.
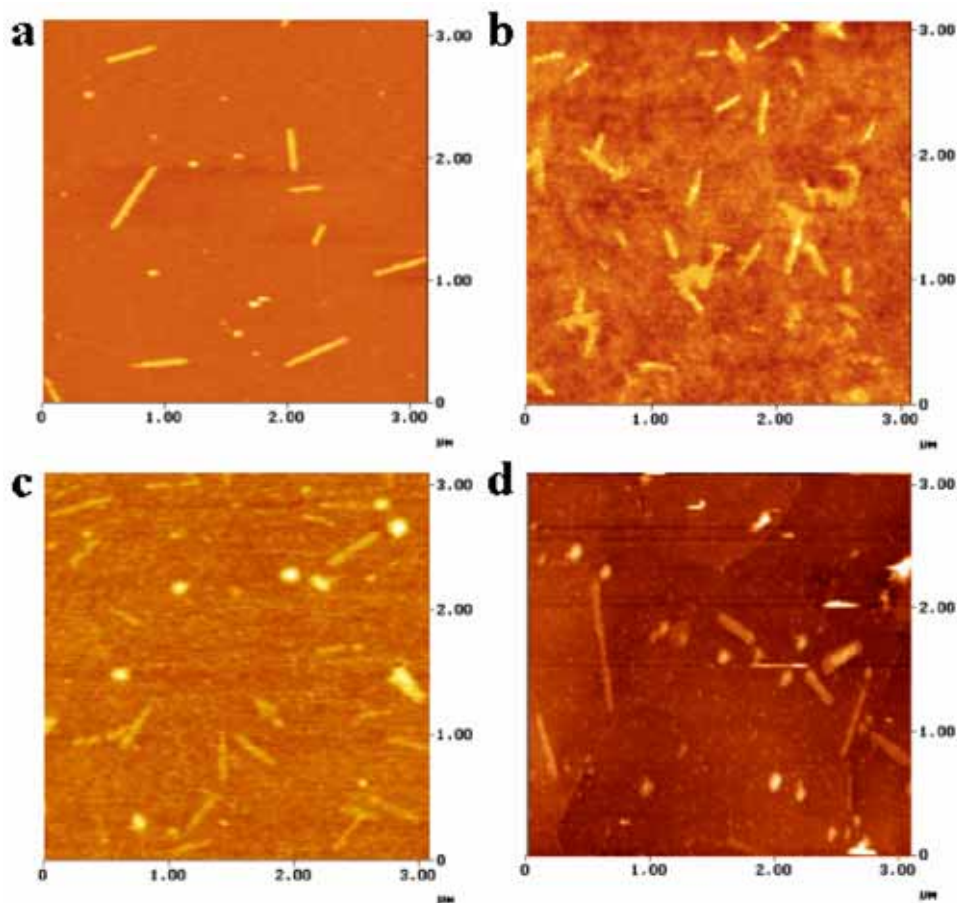

Fig. 5. AFM images of the BPP aggregate deposited from its DMSO solution (2×10^{-5} M) on different substrates: (*a*) mica, (*b*) glass, (*c*) silicon, (*d*) gold (STM image)

The structure of the rod-shaped aggregates, which are deposited on the substrate, changes with the concentration of the stock solution. A series of images, exemplifying this shape evolution process, is represented in *Fig. 6*. As this change in morphology is not accompanied by a spectral change in solution, as was evidenced by UV-VIS absorption spectroscopy (vide supra), it appears that a secondary re-organization on the surface is occurring during the drying process. This implies a coagulation of smaller rod shaped nanocrystals into a larger structure at higher concentrations.
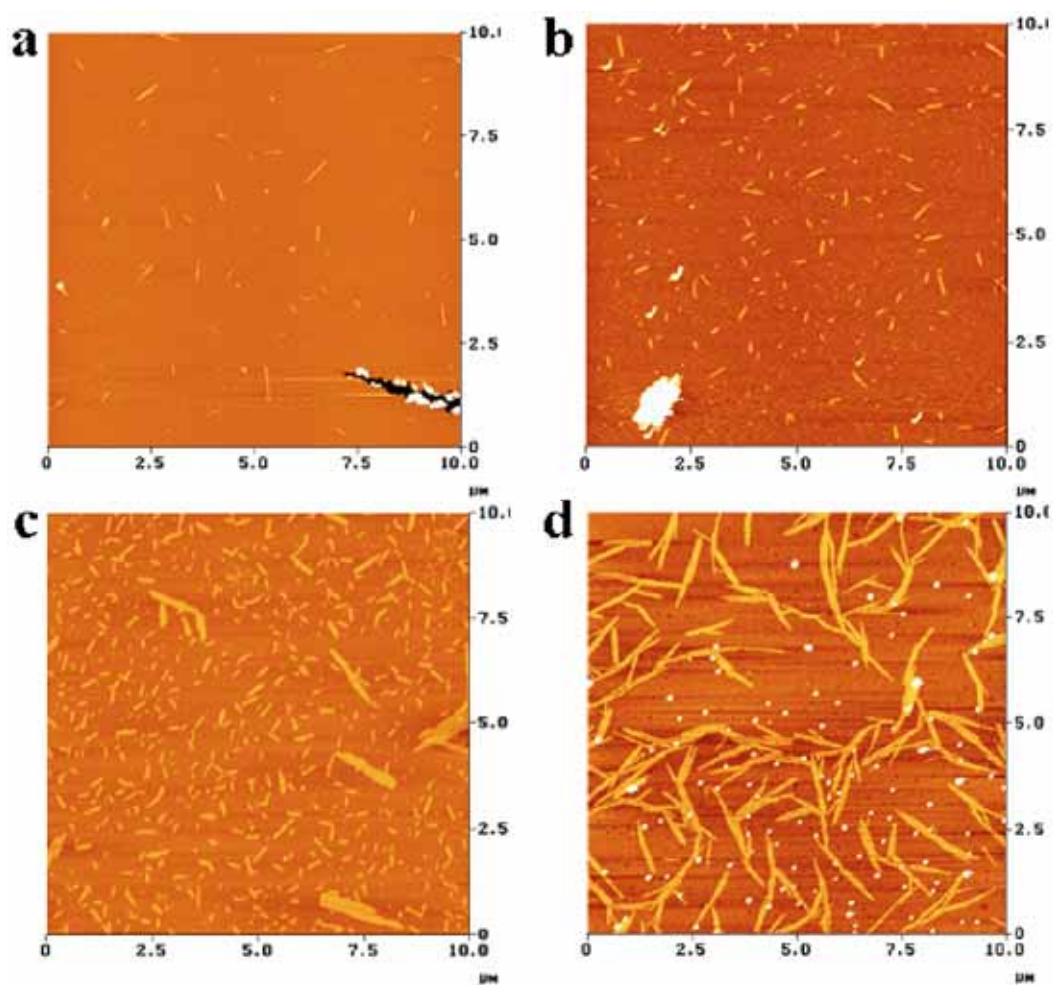
Fig. 6. Structural evolution of the BPP aggregate deposited from its DMSO solution at different concentrations studied with AFM (*a*) 1.6×10^{-5} M, (*b*) 2×10^{-5} M, (*c*) 2.5×10^{-5} M, (*d*) 3.1×10^{-5} M

SNOM and polarized fluorescence images

The strongly red shifted emission from the excitonic state of the nano-rods obtained from DMSO observed at 700 nm, which we had reported previously [13a], allowed us to record Scanning Probe Microscopy images with fluorescence detection. In *Fig. 7* the topographic image and its corresponding fluorescence SNOM image of this aggregate on glass are shown.
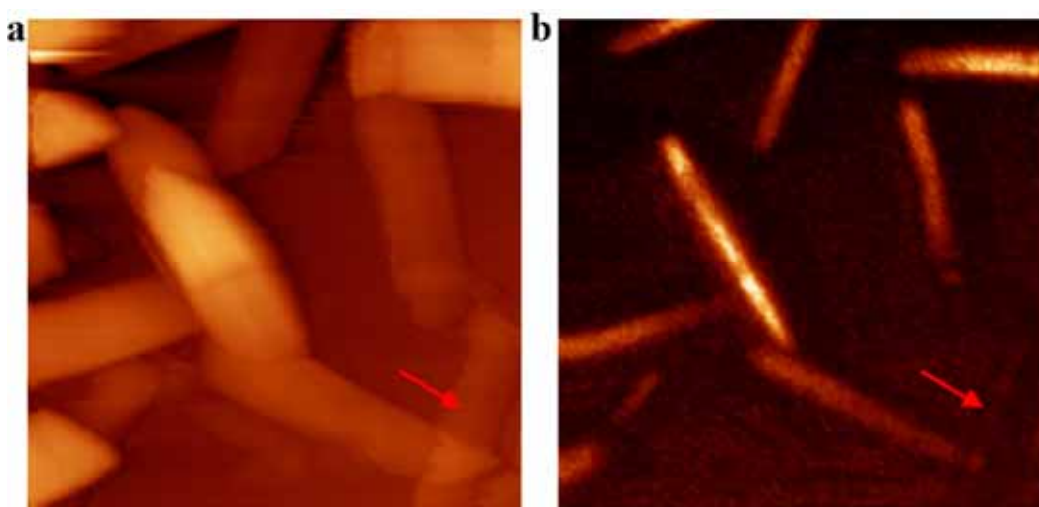
Fig. 7. SNOM images of the aggregates deposited on glass from the DMSO solution (2×10⁻⁵ M): (*a*) a topographic image (size: 5 μm × 5 μm), (*b*) the fluorescence SNOM image (size: 5 μm × 5 μm) collected simultaneously with the topographic image in (*a*)

The SNOM image clearly shows the nano-rod structure of these aggregates. The rod-shaped aggregates observed in the topographic image appear larger than those detected in the fluorescence image due to the tip convolution of the metal coated triangular glass tip used in this experiment [14]. Almost all nano-rods are emissive, and the absence of emission as indicated by the arrow in *Fig. 7* might be due to quenching by the substrate or photo bleaching [17].

Due to difficulty in determining the polarization of the emission in the near field of our triangular tip [14], we measured the polarization of individual aggregates with an optical luminescence microscope [18]. *Figure 8a* displays the fluorescence image of the aggregates recorded by detection of vertically polarized fluorescence, while the horizontally polarized fluorescence is shown in *Fig. 8b*. The angles of polarization were measured by emission-intensity dependence, and the difference between the polarization angle measured by emission and excitation was found to be approximately 0°. We thus conclude that the monomers are stacked one by one inside the nano-rod (*Fig. 8b*, inset) with an angle (θ) between the nano-rod's long axis and the monomer of about 40°.
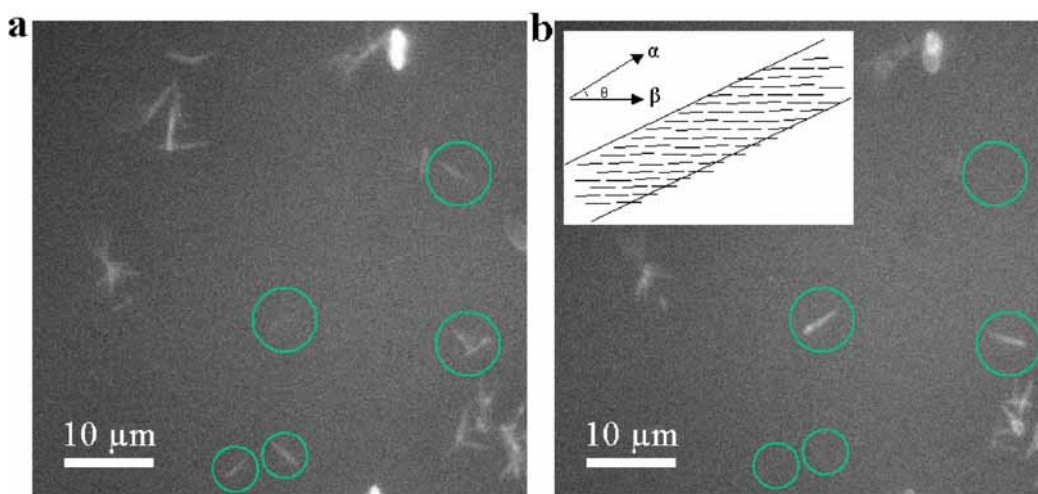
Fig. 8. Photomicrographs showing the luminescence of the aggregates of BPP in *Fig. 7* (upon 532 nm excitation). (*a*) fluorescence polarized vertically to the page and (*b*) fluorescence polarized horizontally to the page. (Inset: cartoon depicting the packing of the monomer inside the nano-rod, α: direction of the long axis of the nano-rod, β: direction of monomer, θ: the angle of α direction relative to β direction)

Internal molecular structure of the nanocrystals

In order to propose a structural model for the packing of the molecules in the rod-shaped aggregates, the information concerning the angle between the orientation of the transition dipole moment of the BPP molecules and the long axis of the nanocrystals may be combined with the previously established data of the closely related *t*-Bu substituted analogue of BPP (*Fig. 9*) [13a].

Figure 9a shows the crystal packing of the *t*-Bu substituted compound. The interaction between two adjacent NH functions in the form of an intramolecular hydrogen bond, and the presence of a hydrogen bond between the solvent (DMSO) and the free NH function as well as the perpendicular orientation of the two adjacent substituents has been described previously [13a]. Assuming that the molecular network in the crystals is similar for the *tert*-butylphenyl substituted BPP investigated in this study, we thus propose a possible stacking arrangement displayed in *Fig. 9b*. This would allow the packing in both longitudinal and lateral direction as indicated in *Fig. 9c*. The role of the phenyl rings in BPP, which sets it apart from the crystallographically characterized derivative, remains unclear but is thought to enhance the intermolecular interactions.
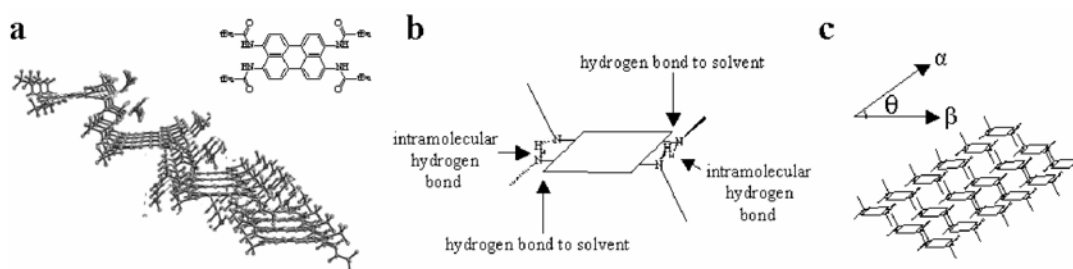
Fig. 9. Elucidation of the molecular packing inside the aggregate: (*a*) crystal structure showing the packing of the *t*Bu substituted analogue of BPP (inset: molecular structure of the *t*Bu substituted perylene); (*b*) proposed intramolecular and intermolecular hydrogen bonding; (*c*) proposed molecular packing inside the nano-rod shaped aggregate

Considering the molecular dimensions (1 × 1 × 2 nm) and the size of the nanocrystals (e.g. 2 × 40 × 250 nm in DMSO and 1 × 20 × 1000 nm in HPMA) it can be concluded that typical nanocrystals formed by BPP contain 10.000 molecules.

Whereas theoretically two molecules can make up a J-aggregate, the well-defined excitonic states in J-type dimers, trimers, tetramers up to decamers can be named more precise. We can assume that typical J-aggregate properties arise above 10 (up to 50) monomers. In general, the typical J-band, attributed to directional orientation of the transition dipoles of the molecules in the aggregate starts to be clearly observed when N is larger than 50. The minimum number of monomers that is needed to form a typical J-aggregate is related to the exciton (diffusion) length. The aggregate length should be as long as the exciton (diffusion) length, which will be influenced by the molecular (monomer) structure. Up to a certain length however, some photophysical properties will still be substantially influenced by the length (and/or width) of the aggregates. For a fixed width, properties (such as the J-band width) will change with $1/\sqrt{N}$ where N is the number of monomers.

Conclusion

In this work we have reported the formation of rod shaped organic nanocrystals in organic media by utilizing self-assembly mechanisms. The aggregational state and the dimension can be controlled by adjusting the hydrogen-bond accepting capacity of the solvent [19], adding hydrogen-bond donors and by varying the concentration. From the results of polarized fluorescence microscopy as well as circumstantial evidence provided

by crystal structure of its *t*-butyl substituted analogue, we propose that the aggregates consist of molecules with intramolecular hydrogen bonds and hydrogen bonding between the free NH functional group and the hydrogen-bond accepting solvents. This leads to a packing pattern with an angle of 40º of the molecular axes relative to the long axis of the nano-rod. The rod shaped nano-aggregates are thermally stable and can be deposited on different substrates, thus making them potential objects for local electronic and photonic transport studies. This may pave the way towards the fabrication of more complicated and functionalized molecular assemblies for new applications.

Acknowledgments

References

[1]   G. Schmid, *Nanoparticles, from theory to application,* Wiley, 2003.

[2]   a) G. Schmid, *Chem. Rev.,* **92**, 1709 (1992). b) Y. G. Sun, Y. N. Xia, *Science,* **298**, 2176 (2002).

[3]   a) J. J. Urban, W. S. Yun, Q. Gu, H. K. Park, *J. Am. Chem. Soc.,* **124**, 1186 (2002). b) T. Trindade, P. O'Brien, N. L. Pickett, *Chem. Mater.,* **13**, 3843 (2001).

[4]   a) A. P. Alivisatos, *Science,* **271**, 933 (1996). b) C. C. Chen, A. B. Herhold, C. S. Johnson, A. P. Alivisatos, *Science,* **276**, 398 (1997). c) M. Bruchez, M. Moronne, P.Gin, S. Weiss, A. P. Alivisatos, *Science,* **281**, 2013 (1998).

[5]   H. Masuhara, H. Nakanishi, K. Sasaki, *Single Organic Nanoparticles*, Springer, 2003.

[6]   N. Rasenack, B. W. Muller, *Pharm. Res.,* **19**, 1894 (2002).

[7]   M. Mas-Torrent, M. Durkut, P. Hadley, X. Ribas, C. Rovira, *J. Am. Chem. Soc.,* **126**, 984 (2004).

[8]   a) W. U. Huynh, J. J. Dittmer, A. P. Alivisatos, *Science,* **295**, 2425 (2002). b) X. F. Duan, Y. Huang, R. Agarwal, C. M. Lieber, *Nature,* **421**, 241 (2003). c) J. Hernando, P. A. J. de Witte, E. van Dijk, J. Korterik, R. J. M. Nolte, A. E. Rowan, M. F. Garcia-Parajo, N. F. van Hulst, *Angew. Chem. Int. Ed.,* **43**, 4045 (2004). d) R. Calarco, M. Marso, T. Richter, A. Aykanat, R. Meijers, A. I. Hart, T. Stoica, H. Luth, *Nano Lett.,* **5**, 981 (2005).

[9]   a) H. Kasai, H. S. Nalwa, H. Oikawa, S. Okada, H. Matsuda, N. Minami, A. Kakuta, K. Ono, A. Mukoh, H. Nakanishi, *Jpn. J. Appl. Phys. Part 2 – Lett.,* **31**, L1132 (1992). b) H. Kasai, H. Kamatani, S. Okada, H. Oikawa, H. Matsuda, H. Nakanishi, *Jpn. J. Appl. Phys. Part 2 – Lett.,* **35**, L221 (1996). c) H. Kasai, H. Kamatani, Y.

Yoshikawa, S. Okada, H. Oikawa, A. Watanabe, O. Itoh, H. Nakanishi, *Chem. Lett.*, **9**, 1181 (1997). d) T. Onodera, T. Oshikiri, H. Katagi, H. Kasai, S. Okada, H. Oikawa, M. Terauchi, M. Tanaka, H. Nakanishi, *J. Cryst. Growth*, **229**, 586 (2001). e) J. I. Niitsuma, T. Fujimura, T. Itoh, H. Kasai, S. Okada, H. Oikawa, H. Nakanishi, *Int. J. Mod. Phys. B*, **15**, 3901 (2001).

[10] a) H. Schoenherr, V. Paraschiv, S. Zapotoczny, M. Crego-Calama, P. Timmerman, C. W. Frank, G. J. Vancso, D. N. Reinhoudt, *Proc. Natl. Acad. Sci. USA*, **99**, 5024 (2002). b) M. Ishi-i, Crego-Calama, P. Timmerman, D. N. Reinhoudt, S. Shinkai, *J. Am. Chem. Soc.*, **123**, 14631 (2002). c) V. Paraschiv, M. Crego-Calama, T. Ishi-i, C. J. Padberg, P. Timmerman, D. N. Reinhoudt, *J. Am. Chem. Soc.*, **124**, 7638 (2002).

[11] F. C. Spano, S. Mukamel, *Phys. Rev. A*, **40**, 5783 (1989).

[12] a) D. A. Higgins, J. Kerimo, D. A. Vanden Bout, P. Barbara, *J. Am. Chem. Soc.*, **118**, 4049 (1996). b) J. L. Seifert, R. E. Connor, S. A. Kushon, M. M. Wang, B. A. Armitage, *J. Am. Chem. Soc.*, **121**, 2987 (1999). c) A. S. R. Koti, N. Periasamy, *Chem. Mater.*, **15**, 369 (2003). d) T. Aktugawa, T. Ohta, T. Hasegawa, T. Nakamura, C. A. Christensen, J. P. Becher, *Proc. Natl. Acad. Sci. USA*, **99**, 5028 (2002). e) P. Samori, V. Francke, K. Muellen, J. P. Rabe, *Thin Solid Film*, **336**, 13 (1998). f) P. Samori, V. Francke, K. Muellen, J. P. Rabe, *Chem. Eur. J.*, **5**, 2312 (1999).

[13] a) L. H. Gade, C. H. Galka, R. M. Williams, L. De Cola, M. McPartlin, B. Dong, L. F. Chi, *Angew. Chem. Int. Ed.*, **42**, 2677(2003). b) K. W. Hellmann, C. H. Galka, I. Rüdenauer, L. H. Gade, I. J. Scowen, M. McPartlin, *Angew. Chem. Int. Ed.*, **37**, 1948 (1998). c) L. H. Gade, C. H. Galka, K. W. Hellmann, R. M. Williams, L. De Cola, I. J. Scowen, M. McPartlin, *Chem. Eur. J.*, **8**, 3732 (2002).

[14] A. Naber, D. Molenda, U. C. Fischer, H. J. Maas, C. Hoeppener, N. Lu, H. Fuchs, *Phys. Rev. Lett.*, **89**, 210801 (2002).

[15] a) H. Yao, S. Sugiyama, R. Kawabata, H. Ikeda, O. Matsuoka, S. Yamamoto, N. Kitamura, *J. Phys. Chem. B.*, **103**, 4452 (1999). b) S. Sugiyama Ono, H. Yao, O. Matsuoka, R. Kawabata, N. Kitamura, S. Yamamoto, *J. Phys. Chem. B.*, **103**, 6909 (1999). c) H. Von Berlepsch, C. Boettcher, *J. Phys. Chem. B.*, **106**, 3146 (2002). d) H. Von Berlepsch, S. Kirstein, C. Boettcher, *Langmuir*, **18**, 7699 (2002).

[16] a) I. Struganova, *J. Phys. Chem. A.*, **104**, 9670 (2000). b) M. M. Wang, G. L. Silva, B. A. Armitage, *J. Am. Chem. Soc.*, **122**, 9977 (2000).

[17] D. A. Higgins, P. F. Barbara, *J. Phys. Chem.*, **99**, 3 (1995).

[18] a) J. E. Maskasky, *Langmuir*, **7**, 407(1991). b) D. A. Higgins, P. J. Reid, P. F. Barbara, *J. Phys. Chem.*, **100**, 1174 **(**1996)

[19] For H-bond acceptor strengths see, C. A. Hunter, *Angew. Chem. Int. Ed.*, **43**, 5310 (2004).